

Shock wave measurements in cloud cavitation

G.E. Reisman, C.E. Brennen

Department of Mechanical Engineering, California Institute of Technology, Pasadena, California 91125, USA

Abstract: One of the most destructive (and noisy) forms of cavitation is that referred to as “**cloud cavitation**” because it involves a large collection of bubbles which behave as a coherent whole. The present paper presents the results of an experimental study of the processes of collapse of a cavitation bubble cloud, specifically that generated by an oscillating hydrofoil in a water tunnel. Measurements of the far-field noise show that this is comprised of substantial pulses radiated from the cloud at the moment of collapse. Also, transducers within the cavitation zone encounter very large pressure pulses (or shock waves) with amplitudes of the order of tens of atmospheres and typical durations of the order of tenths of a millisecond. These shock waves appear to be responsible for the enhanced noise and damage potential which results from that phenomenon.

Key words: Cloud cavitation, Shock Waves, Hydrofoil, Pressure Transducers, High-speed motion pictures

1. Introduction

Clouds of cavitation bubbles which grow and collapse coherently are known to be particularly noisy and destructive (see, for example, Knapp (1955), Bark and van Berlekom (1978), Soyama *et al.* (1992)). This violence went largely unexplained until the 1980s when Mørch, Kedrinskii and co-workers (1980, 1981) suggested that cloud collapse begins with bubble collapse on the surface of the cloud and is followed by an inwardly propagating shock wave which grows in magnitude due to geometric focussing. Recently, we have carried out numerical calculations of the collapse of a spherical cloud (Wang and Brennen (1995), (1996)) which confirmed this view and allowed identification of the parametric regimes in which this shock-focussing effect occurs. The shock waves themselves have a structure very similar to the shock structures observed and calculated by Noordzij and van Wijngaarden (1974) (and, more recently, Kameda and Matsumoto (1995)) for gas/liquid mixtures. The calculations of Wang and Brennen showed that the cloud collapse dynamics are highly dependent on the “cloud interaction” parameter, β , defined by $\alpha A^2/R^2$ where α and A are respectively the initial void fraction and radius of the cloud and R is the initial bubble radius. Only when β is much larger than unity do shock waves form, propagate and focus during collapse. Smaller values lead to a much more benign behavior in which bubble collapse

starts in the center of the cloud.

Of course, actual bubble clouds are usually far from spherical and therefore exhibit more complicated shock-focussing mechanisms (qualitatively similar to those described by Sturtevant and Kulkarny (1976) in single phase flows) at large β . It seems likely that the focussing will produce smaller magnitude pulses the further one departs from the spherical geometry.

The present paper presents the results of an experimental study of the processes of collapse of a real bubble cloud, specifically that generated by an oscillating hydrofoil in a water tunnel. Not only is this a fairly simple way to produce a cavitation cloud but the results have real practical value for cloud cavitation on ship propeller blades or pump impeller blades is common and leads to serious problem. While there have been a number of previous experimental studies of cloud cavitation on hydrofoils (most notably by Bark and Berlekom (1978), Shen and Peterson (1978), Bark (1985), Kubota *et al.* (1989), and Reisman *et al.* (1994)), none have looked closely for propagating shock waves within the bubble cloud.

2. Experiments

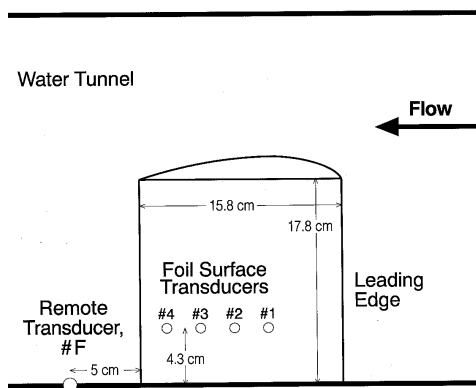


Figure 1. Schematic of the foil and the pressure transducers in the water tunnel.

We describe here experimental observations of cloud cavitation generated by oscillating a hydrofoil in a water tunnel (Reisman (1997)). The resulting growth and collapse of the cavitation on the suction surface is studied using high speed movies and correlating the structure of the cavitation with measurements of the impulsive pressures within the cloud (and radiated away from it).

Finite span hydrofoils of chord, $c = 15.2\text{cm}$ and span, $s = 17.5\text{cm}$, were reflection-plane mounted in the floor of a water tunnel (Reisman (1997)), set at a given mean angle of incidence, $\bar{\alpha}_f$ (usually 5°), and oscillated in pitch with an amplitude, usually $\pm 5^\circ$, and a radian frequency, Ω , quoted in terms of a reduced frequency, $k = \Omega c/2U$.

The unsteady pressures generated by the cavitation on the hydrofoil were measured by (1) four PCB model 105B02 pressure transducers (flat frequency response to 50kHz , face diameter about 3mm) denoted by #1 through #4 which were recess-mounted on the suction surface of the foil as shown in Fig. 1 and (2) a PCB model HS113A21 piezo-electric pressure transducer (denoted by #F) with a flat frequency response up to 100kHz flush-mounted flush in the floor of the test section. These were calibrated as described in Reisman (1997). In addition, high speed movies with a framing rate of 500fps were taken of the cavitation and were correlated with the pressure transducer output to determine the structures in the cavitation which led to the pressure transients detected.

3. Stages of the cavitation cycle

Detailed descriptions of cavity growth, collapse and cloud formation on hydrofoils have been given by many authors including Knapp (1955), Wade and Acosta (1966), Bark (1985), McKenney and Brennen (1994), Shen and Peterson (1978, 1980), Franc and Michel (1988), Hart et al. (1990), Kubota et al. (1989,1992), Le et al. (1993), de Lange et al. (1994) and Kawanami et al. (1996). By viewing the high speed motion pictures taken during the current experiments, a series of stages in the cloud cavitation process were identified. These are depicted schematically in Fig. 2 for a single foil oscillation cycle.

During that part of the oscillation cycle when the instantaneous angle of attack, α_f , is increasing, cavitation inception occurs in the tip vortex and is soon followed by traveling bubble cavitation in the region of minimum pressure. As the angle of attack increases further, the bubbles coalesce into a single attached cavitation sheet which attains its maximum length as the angle of attack reaches a maximum. Near the end of this process, the re-entrant liquid jet (previously noted by Knapp (1955), Wade and Acosta (1966) and others) penetrates the attached cavity from downstream and flows forward on the foil surface. It does not, however, progress uniformly toward the leading edge. The jet penetration is maximum at approximately 30% span (from the base of the foil) as depicted in sketches (a), (b), (c) and (d) of Fig. 2. These sketches correspond to the moments in the cycle at which $\alpha_f = 10^\circ, 8.4^\circ, 6.9^\circ$ and 5.4° respectively.

The current observations indicate, however, that the

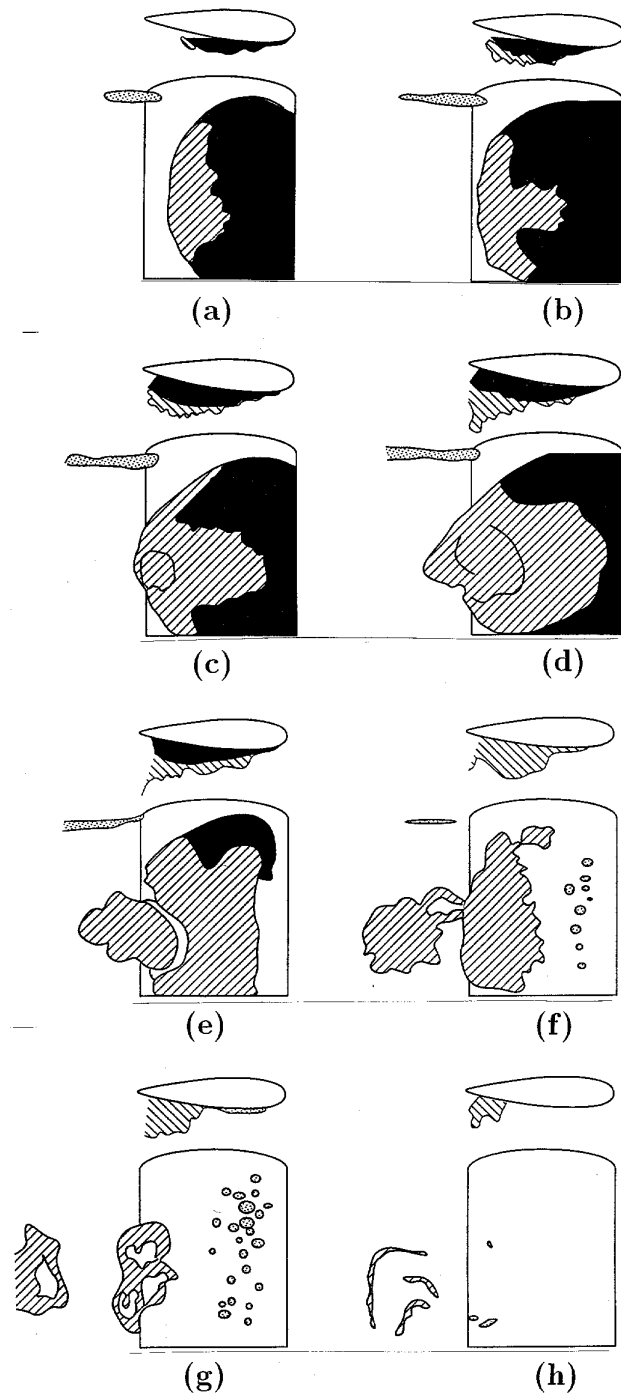


Figure 2. Profile and planform sketches of the cloud cavitation as traced from high speed motion pictures of a single foil oscillation cycle. Shaded areas - sheet cavitation; hatched areas - bubbly mixture; dotted areas - traveling bubble or tip vortex cavitation. NACA 0021 foil oscillating at $k = 0.7$, $\sigma = 0.9 - 0.95$, $U = 8.5\text{m/s}$, $\bar{\alpha}_f = 7^\circ$.

processes which occur *after* the passage of the re-entrant jet are critical. The large pressure pulses on the foil surface, which will be described in greater detail below, were detected only after the re-entrant jet had passed the

measurement location. As it progresses, the jet breaks the attached sheet cavity up into a bubbly mixture. The thickness of the bubbly mixture increases in the region through which the jet passes by a mixing of the vapor/gas contained in the cavity with the surrounding liquid to create a larger volume of bubbly liquid. Finally, the remains of the sheet cavity form a cloud of bubbles that undergoes a coherent collapse as it is convected into a region of higher pressure near the foil trailing edge as depicted in sketches (d), (e), (f) and (g) of Fig. 2 during which time α_f decreases from 5.4° to the minimum of 2° and increases again to 4.7° . Two frames on either side of cloud collapse are shown in the photographs of Fig. 4. Note that it results in only a slight change in the cloud radius; instead there is a large change in the void fraction inside the cloud.

4. Transducer signals

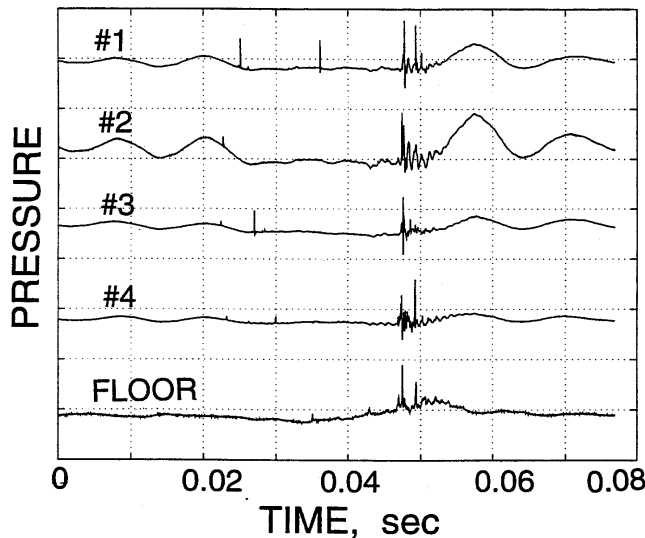


Figure 3. Typical signals from transducers #1-#4 and #F during a single oscillation cycle of the NACA 0021 foil. The vertical scale is 1 MPa/div. for the foil surface transducers, #1-#4, and 100 kPa/div. for the floor transducer, #F. Data for $\sigma = 0.95$, $k = 0.78$, $U = 8 \text{ m/s}$ and $\bar{\alpha}_f = 5^\circ$.

Simultaneous transducer recordings and high speed motion pictures were acquired for two different foils over a range of flow conditions (cavitation number, σ , tunnel velocity, U , mean angle of incidence, $\bar{\alpha}_f$ and water air content), reduced frequencies, k , and oscillation amplitudes (Reisman (1997)). A typical set of output signals from the transducers is shown in Fig. 3; this shows a single foil oscillation cycle with the origin corresponding to the maximum angle of attack. The broad, low-frequency variations in these transducer signals are not pressures in the water; instead we focus on the sharp pulses in these records which are illustrative of pressure pulses caused by cavitation. Note that the pulses in the foil surface transducers are *large* with typical magnitudes as large

as 10 bar and durations of the order of 10^{-4} s . These are certainly sufficient to explain the enhanced noise and cavitation damage associated with cloud cavitation. The floor transducer is indicative of the noise radiated by the cavitation; its magnitude declines with distance from the cavitation.

5. Correlation with cavitation structures

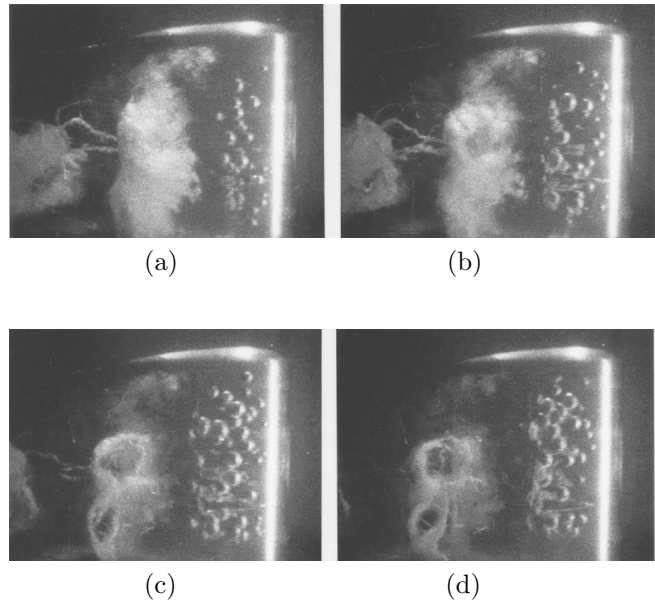
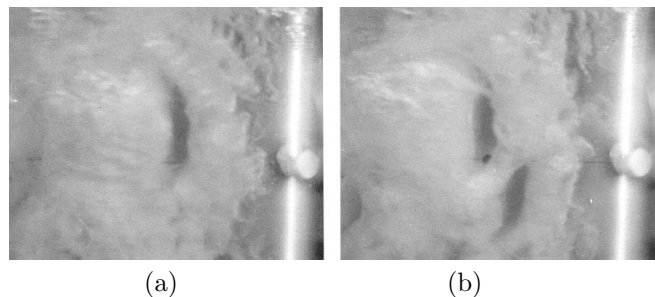


Figure 4. Consecutive high speed movie frames (2 ms apart) showing global cloud collapse. The flow parameters are $\sigma = 0.95$, $k = 0.71$, $U = 8.5 \text{ m/s}$ and $\bar{\alpha}_f = 7^\circ$.

Two distinct types of pulse were evident in the transducer signals and correlation of the signals with the movies revealed that each is associated with a particular type of event or structure within the cavitating cloud.



One type of pulse, known as a *global* pulse or event, is associated with the coherent collapse of a bubble cloud when it separates from the rear of the cavitating region and is convected into a region of higher pressure. This type of structure causes the largest impulsive pressures and radiated noise. The pulses it produces are termed *global* pulses since they are recorded almost simultaneously by all transducers; an example is the event at about 0.047 sec in Fig. 3. Figure 4 depicts four consecutive

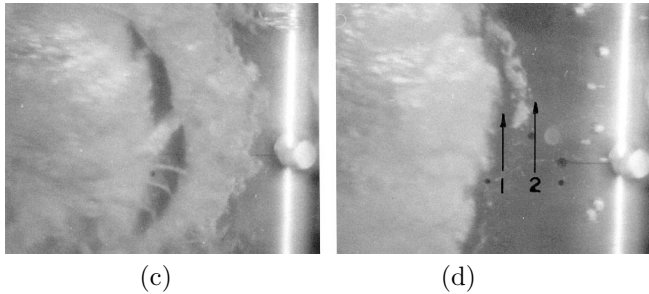


Figure 5. Local pulse structures in the cavitation on the suction surface of the NACA 0021 foil at $\sigma = 0.9$, $k = 0.71$, $U = 8.5\text{m/s}$ and $\bar{\alpha}_f = 7^\circ$. The flow is from right to left; the field of view includes the four transducer locations and the leading edge is just at the right border. Crescent-shaped structures are seen in (a), (b), and (c) and a leading edge event with two collapses (indicated by the arrows labelled 1 and 2) is seen in photograph (d).

frames from a movie of such an event; the cavitation cloud which is the remnant of the attached sheet cavity undergoes a rapid and coherent collapse between frames (b) and (c) of this figure. The collapse of this region radiates a pressure pulse which is detected by all the transducers. Note from Fig. 4, that global cloud collapses do not involve large changes in the overall dimensions of the cloud. Rather collapse involves large changes in the void fraction distribution within the cloud, a feature which is consistent with the calculations of Wang and Brennen (1995, 1996).

But, unexpectedly, two other types of structures were observed. Typically, their pulses are recorded by only one transducer and these events are therefore called *local* pulses; several can be observed in Fig. 3 between 0.025sec and 0.04sec . They occur when a bubbly shock wave structure within the cavitation passes over the face of a transducer. While these *local* events are smaller and therefore produce less radiated noise than the global events, the pressure pulse magnitudes are almost as large. The two types of structures which are observed to caused local pulses are termed “crescent-shaped regions” and “leading edge structures”; both occur during the less coherent collapse of clouds.

The first type of flow structure (illustrated in photographs (a) through (c) of Fig. 5) is a crescent-shaped region of low void fraction. These crescent-shaped regions appear randomly in the bubbly mixture which remains after the passage of the reentrant jet. A close look at photograph (c) shows how complicated these flow structures can be since this crescent-shaped region appears to have some internal structure. Photographs (b) and (c) also show that more than one crescent-shaped structure can be present at any moment in time.

In addition, the movie and pressure data consistently displayed a local pulse when the upstream boundary, or

leading edge, of the detached bubbly mixture passed over a transducer. This second type of local flow structure (which also produces a local pulse) is illustrated in photograph (d) of Fig. 5. These “leading edge structures” are created when the sheet cavity detaches from the foil and they propagate downstream faster than the mixture velocity.

6. Other features of global pulses

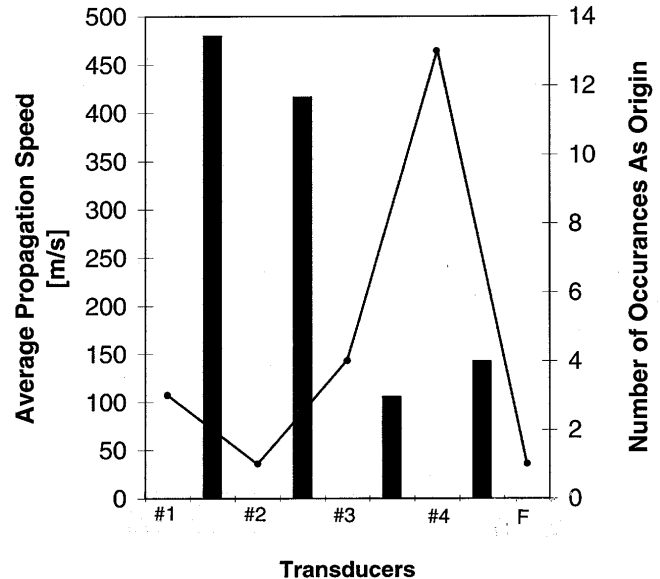


Figure 6. Speed of propagation (vertical bars) and location of the origin of the global pressure pulses (line). Data for $\sigma = 0.95$, $k = 0.76$, $U = 8\text{m/s}$, and $\bar{\alpha}_f = 5^\circ$.

By examining the time delays in the global pulse signals from the five transducers, it was possible to extract some information on the location of the origin of the global pulses and on the speeds of propagation of those pulses through the inhomogeneous environment which exists near the surface of the hydrofoil at the time of the global cloud collapse.

The transducer signals for 41 global pulse events, all at one representative flow condition, were analysed. The location of the origin of the global pulses could be estimated by noting, for each event, the transducer which first registers the global pressure pulse. The number of events (out of 41) for which the origin could be so identified is shown in Fig. 6. We note that global pulses most frequently originated near transducer #4 which is consistent with the high speed movie observations at this operating condition.

Furthermore, the speed of propagation of the global pressure pulse could be calculated from the time intervals separating the arrival of pulses at neighbouring transducers. These time intervals were converted to propagation speeds and are presented by the vertical bars in Fig. 6.

In all cases, the propagation speeds are a small fraction of the sonic speed in either the pure liquid or pure vapor phase. The speeds for the rear intervals on the foil are substantially slower than the speeds for the forward intervals perhaps because, at the moment of cloud collapse, there is a sharp increase in the void fraction downstream of the #3 transducer. This is due to the fact that the bubbly remains of the sheet cavity have been convected to this location at that moment in time.

But these speeds represent the rates at which the acoustic pulses are propagated *away from* the cloud. It is also of interest to estimate the speed of propagation of the collapse process inside the cavitation cloud. The final stage of global cloud collapse proceeds very rapidly as was demonstrated in frames (b) and (c) of Fig. 4. The collapse process propagates through the cloud, a distance of about 6cm, between frames (b) and (c) which are separated by 2ms. Thus a crude lower bound on the collapse propagation speed is 30m/s; the actual collapse could well travel much faster.

7. Conclusions

Recent numerical calculations of the growth and collapse of a spherical cloud of cavitation bubbles by Wang and Brennen (1994, 1995) have demonstrated that, provided the cloud interaction parameter, β , is large enough, collapse occurs first on the surface of the cloud as earlier suggested by Mørch, Kedrinskii and their co-workers. The inward propagating collapse front then becomes a bubbly shock wave which grows in magnitude due to geometric focussing. Very large pressures and radiated impulses occur when the shock reaches the center of the cloud. Of course, actual clouds are far from spherical and, even in a homogeneous medium, gasdynamic shock focussing can be quite complex and involve significant non-linear effects (see, for example, Sturtevant and Kulkarny (1976)). Nevertheless, it seems evident that once collapse is initiated on the surface of a cloud, the propagating shock will focus and produce large local pressure pulses and radiated acoustic pulses.

Experiments with hydrofoils experiencing cloud cavitation have shown that very large pressure pulses occur within the cloud and are radiated away from it during the collapse process. Within the cloud, these pulses can have magnitudes as large as 10bar and durations of the order of 10^{-4} s. These are certainly sufficient to explain the enhanced noise and cavitation damage associated with cloud cavitation. Moreover, these pressure pulses are associated with several distinct shock structures which can be observed visually and which propagate through the bubbly mixture.

Thus we suggest a new perspective on cavitation damage and noise in flows which involve large collections of

cavitation bubbles with a sufficiently large void fraction (or, more specifically, a large enough β) so that the bubbles interact and collapse coherently. This view maintains that the cavitation noise and damage is generated by the formation and propagation of bubbly shock waves within the collapsing cloud. The experiments reveal several specific shock wave structures. One of these is the mechanism by which the large coherent collapse of a finite cloud of bubbles occurs. A more unexpected result was the discovery of more localized bubbly shock waves propagating within the bubbly mixture in several forms, as crescent-shaped regions and as leading edge structures. These seem to occur when the behavior of the cloud is less coherent. They produce surface loadings which are within an order of magnitude of the more coherent events and could also be responsible for cavitation damage. However, because they are more localized, the radiated noise they produce is much smaller than that due to global events.

The ubiquity and severity of these propagating shock wave structures provides a new perspective on the mechanisms responsible for noise and damage in cavitating flows involving clouds of bubbles. It would appear that shock wave dynamics rather than the collapse dynamics of single bubbles determine the damage and noise in many cavitating flows. And this may suggest new ways of modifying cavitation noise and damage.

Acknowledgement. The authors are very grateful for the support for this research provided by the Office of Naval Research under Contract N00014-91-J-1295.

References

- Bark G and Berlekom WB (1978) Experimental investigations of cavitation noise. Proc 12th ONR Symp on Naval Hydrodynamics, pp470-493.
- Bark G (1985) Developments of distortions in sheet cavitation on hydrofoils. Proc ASME Int Symp on Jets and Cavities, pp470-493.
- de Lange DF, de Bruin GJ and van Wijngaarden L (1994) On the mechanism of cloud cavitation - experiment and modeling. Proc 2nd Int Symp on Cavitation, pp45-50.
- Franc JP and Michel JM (1988) Unsteady attached cavitation on an oscillating hydrofoil. J Fluid Mech 193:171-189.
- Hanson I, Kedrinskii VK and Mørch KA (1981) On the dynamics of cavity clusters. J Appl Phys 15:1725-1734.
- Hart DP, Brennen CE and Acosta AJ (1990) Observations of cavitation on a three dimensional oscillating hydrofoil. ASME Cavitation and Multiphase Flow Forum, FED-Vol. 98: 49-52.
- Kameda M and Matsumoto Y (1996) Structure of

- shock waves in a liquid containing gas bubbles. Proc IUTAM Symp on Waves in Liquid/Gas and Liquid/Vapor Two-Phase Systems:117-126.
- Kawanami Y, Kato H, Yamaguchi H, Tagaya Y and Tamimura M (1996) Mechanism and control of cloud cavitation. Proc ASME Symp on Cavitation and Gas-Liquid Flows in Fluid Machinery and Devices, FED-Vol. 236: 329-336.
- Knapp RT (1955) Recent investigations of the mechanics of cavitation and cavitation damage. Trans ASME 77: 1045-1054.
- Kubota A, Kato H, Yamaguchi H and Maeda M (1989) Unsteady structure measurement of cloud cavitation on a foil section using conditional sampling. ASME J Fluids Eng 111:204-210.
- Le Q, Franc JM and Michel JM (1993) Partial cavities: global behaviour and mean pressure distribution. ASME J Fluids Eng 115: 243-248.
- McKenney EA and Brennen CE (1994) On the dynamics and acoustics of cloud cavitation on an oscillating hydrofoil. Proc ASME Symp on Cavitation and Gas-Liquid Flows in Fluid Machinery and Devices, FED-Vol.190: 195-202.
- Mørch KA (1980) On the collapse of cavity cluster in flow cavitation. Proc First Int Conf on Cavitation and Inhomogenities in Underwater Acoustics, Springer Series in Electrophysics 4:95-100.
- Mørch KA (1981) Cavity cluster dynamics and cavitation erosion. Proc ASME Cavitation and Polyphase Flow Forum, pp1-10.
- Noordij L and van Wijngaarden L (1974) Relaxation effects, caused by relative motion, on shock waves in gas-bubble/liquid mixtures. J Fluid Mech 66:115-143.
- Reisman GE, McKenney EA and Brennen CE (1994) Cloud cavitation on an oscillating hydrofoil. Proc 20th ONR Symp on Naval Hydrodynamics, pp78-89.
- Reisman GE (1997) Dynamics, acoustics and control of cloud cavitation on hydrofoils. PhD thesis, Cal Inst of Tech.
- Shen Y and Peterson FB (1978) Unsteady cavitation on an oscillating hydrofoil. Proc 12th ONR Symp on Naval Hydrodynamics, pp362-384.
- Shen Y and Peterson FB (1980) The influence of hydrofoil oscillation on boundary layer transition and cavitation noise. Proc 13th ONR Symp on Naval Hydrodynamics, pp221-241.
- Soyama H, Kato H and Oba R (1992) Cavitation observations of severely erosive vortex cavitation arising in a centrifugal pump. Proc Third IMechE Int Conf on Cavitation, pp103-110.
- Sturtevant B and Kulkarny VJ (1976) The focussing of weak shock waves. J Fluid Mech 73:651-680.
- Wade RB and Acosta AJ (1966) Experimental observations on the flow past a plano-convex hydrofoil. ASME J Basic Eng 88: 273-283.
- Wang Y-C and Brennen CE (1994) Shock wave development on the collapse of a cloud of bubbles. Cavitation and Multiphase Flow Forum, FED 194:15-19.
- Wang Y-C and Brennen CE (1995) The noise generated by the collapse of a cloud of cavitation bubbles. Joint ASME/JSME Fluids Eng Ann Conf, August 1995, Hilton Head Island, SC, USA.

▷ [PREVIOUS PAPER](#)

▷ [NEXT PAPER](#)

▷ [CURRENT LOCATION IN TABLE OF CONTENTS](#)

▷ [CURRENT LOCATION IN REFERENCE NUMBER INDEX](#)

▷ [TOP OF TABLE OF CONTENTS](#)

▷ [TOP OF KEYWORDS INDEX](#)

▷ [TOP OF AUTHOR INDEX](#)

▷ [TOP OF REFERENCE NUMBER INDEX](#)